

Special Issue

Lateral Metallation and Redistribution Reactions of Sodium Ferrates Containing Bulky 2,6-Diisopropyl-*N*-(trimethylsilyl)anilide Ligands

 Lewis C. H. Maddock,^[a] Rebekka Morton,^[b] Alan R. Kennedy,^[b] and Eva Hevia^{*[a]}

Abstract: Alkali-metal ferrates containing amide groups have emerged as regioselective bases capable of promoting Fe–H exchanges of aromatic substrates. Advancing this area of heterobimetallic chemistry, a new series of sodium ferrates is introduced incorporating the bulky arylsilyl amido ligand N(SiMe₃)(Dipp) (Dipp = 2,6-*i*-Pr₂-C₆H₃). Influenced by the large steric demands imposed by this amide, transamination of [NaFe(HMDS)₃] (HMDS = N(SiMe₃)₂) with an excess of HN(SiMe₃)(Dipp) led to the isolation of heteroleptic [Na(HMDS)₂Fe{N(SiMe₃)Dipp}]_∞ (1) resulting from the exchange of just one HMDS group. An alternative co-complexation approach, combining the homometallic metal amides [NaN(SiMe₃)Dipp] and [Fe{N(SiMe₃)Dipp}]₂ induces lateral metal-

lation of one Me arm from the SiMe₃ group in the iron amide furnishing tetrameric [NaFe{N(SiMe₃)Dipp}{N(SiMe₃)Dipp}]₄ (2). Reactivity studies support that this deprotonation is driven by the steric incompatibility of the single metal amides rather than the basic capability of the sodium reagent. Displaying synergistic reactivity, heteroleptic sodium ferrate 1 can selectively promote ferration of pentafluorobenzene using one of its HMDS arms to give heterotrileptic [Na{N(SiMe₃)Dipp}(HMDS)Fe(C₆F₅)]_∞ (4). Attempts to deprotonate less activated pyridine led to the isolation of NaHMDS and heteroleptic Fe(II) amide [(py)Fe{N(SiMe₃)Dipp}(HMDS)] (5), resulting from an alternative redistribution process which is favoured by the Lewis donor ability of this substrate.

Introduction

Stable, two-coordinate open-shell iron complexes continue to attract widespread interest due to their unique structural and magnetic properties.^[1] Amongst this family of compounds iron *bis*(amide) [Fe(HMDS)₂]₂, having relatively basic bulky silylamido substituents, has become a versatile precursor to access a variety of Fe(II) compounds. Some of its applications include the fundamental exploration of its coordination chemistry and associated molecular magnetism,^[2–7] the synthesis of hydride clusters,^[8,9] hydrosilylation catalysis,^[10] as well as emerging as an excellent precursor to access elusive low-coordinate Fe(I) anionic species.^[11] Exhibiting a dimeric solid-state structure, [Fe(HMDS)₂]₂ exists as a linear two-coordinate monomer in

solution in non-donor solvents at ambient temperature.^[12] Power reported the synthesis and structure of two-coordinate [Fe{N(SiMe₃)Dipp}]₂^[13,14] with its more bulky amide, for which DFT calculations has shown that dispersion forces play a key role in the stabilization of its monomeric structure.^[14] While the chemistry of this iron amide has been significantly less explored than that of its HMDS congener, it has been found to undergo reduction using KC₈ furnishing potassium Fe(I) ferrate species^[15,16] or NHC-stabilized heteroleptic two-coordinate Fe(I) complexes.^[17,18] The latter complexes can effectively catalyse cyclotrimerisations of terminal and internal alkynes.^[17,19]

Recent studies by our group and others have shown that combining iron(II) amides (or alkyls) with a group 1 metal reagent lead to the formation of bimetallic bases (via co-complexation) capable of promoting Fe–H exchange reactions of different aromatic substrates.^[20–24] Notably, Klett, Mulvey and co-workers have reported a powerful Na/Fe amide combination capable of regioselective 1,4-dideprotonation of benzene.^[20] Knochel has detailed a trimetallic system formulated as (TMP)₂Fe·MgCl₂·2 LiCl (TMP = 2,2,6,6-tetramethylpiperidine) for the ferration of a variety of substituted arenes, which in turn undergo cross-couplings with aryl halides.^[21] Through our own investigations we have found homoleptic sodium ferrates [MFe(HMDS)₃] (M = Li, Na) particularly effective for *ortho*-metallation of sensitive, activated fluoroarenes.^[22,24] While structural studies confirm that the products of these reactions are formally the result of a direct Fe–H exchange, recent mechanistic studies^[23] have proposed a cooperative pathway where initially sodiation of the substrate takes place, followed by fast transmetallation to Fe forming more covalent Fe–C bonds that stabilise the sensitive aryl fragments. Since this process occurs in a bimetallic

[a] Dr. L. C. H. Maddock, Prof. Dr. E. Hevia
 Department für Chemie, Biochemie und Pharmazie
 Universität Bern
 Freiestrasse 3, 3012 Bern (Switzerland)
 E-mail: eva.hevia@dcb.unibe.ch

[b] R. Morton, Dr. A. R. Kennedy
 WestCHEM, Department of Pure and Applied Chemistry
 University of Strathclyde
 295 Cathedral St, Glasgow, G1 1XL (UK)

Supporting information for this article is available on the WWW under <https://doi.org/10.1002/chem.202102328>

This manuscript is part of a Special Issue “Cooperative effects in heterometallic complexes”.

© 2021 The Authors. Chemistry - A European Journal published by Wiley-VCH GmbH. This is an open access article under the terms of the Creative Commons Attribution Non-Commercial NoDerivs License, which permits use and distribution in any medium, provided the original work is properly cited, the use is non-commercial and no modifications or adaptations are made.

structure it has been coined intramolecular *trans*-metal-trapping.^[25] Interestingly, modifying the amide substituents in the ferrate base can finely tune its reactivity. Thus, replacing one HMDS of the sodium ferrate by a more basic TMP group, ferration of non-activated arenes including benzene, toluene and pyridine was observed. Adding a new level of complexity to these transformations, computational studies suggest that heteroleptic $[\text{NaFe}(\text{TMP})(\text{HMDS})_2]$ can undergo ligand redistribution processes, not unlike Schlenk equilibria found for $\text{Mg}(\text{II})$ reagents, giving rise to the simultaneous presence of several sodium ferrate species in solution.

Building on this background, here we extend our studies to arylsilyl amide ligand $[\text{N}(\text{SiMe}_3)(\text{Dipp})]$, assessing the effects imposed by its large steric demands to the bimetallic cooperativity of sodium ferrates and their applications to promote Fe–H exchange processes using fluorobenzene and pyridine as model substrates.

Results and Discussion

Preparing sodium ferrates with $\text{N}(\text{SiMe}_3)\text{Dipp}$ ligands

We started investigations attempting the preparation of homoleptic *tris*(amide) $[\text{NaFe}\{\text{N}(\text{SiMe}_3)\text{Dipp}\}_3]$. Building on our previous studies which have shown the ability of $[\text{NaFe}(\text{HMDS})_3]$ (I) to undergo transamination with dipyrindylamine,^[26] we first probed this approach by reacting I with 3 equivalents of $\text{HN}(\text{SiMe}_3)\text{Dipp}$ (Figure 1). The reaction mixture was heated under reflux in hexane for one hour affording an orange solution that on cooling furnished crystals of heteroleptic $[\text{Na}(\text{HMDS})_2\text{Fe}\{\text{N}(\text{SiMe}_3)\text{Dipp}\}]_\infty$ (1) in a 22% isolated crystalline yield. Surprisingly, despite the excess of amine and the relatively forcing conditions applied, only one amide group of I undergoes transamination. Alternatively, 1 could also be

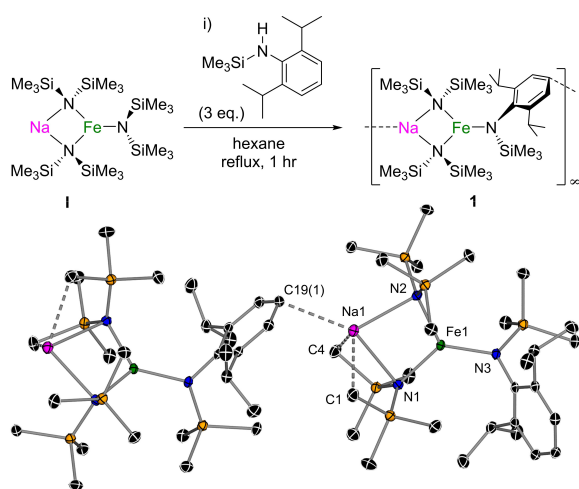
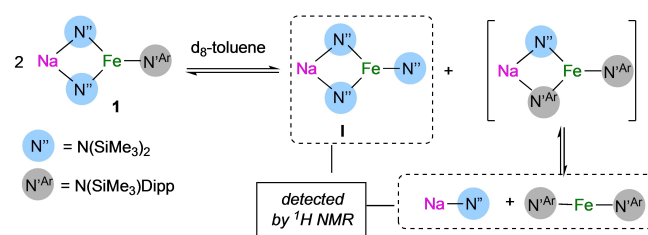


Figure 1. Synthesis of $[\text{Na}(\text{HMDS})_2\text{Fe}\{\text{N}(\text{SiMe}_3)\text{Dipp}\}]_\infty$ (1) and a section of its polymeric structure in the crystal. Ellipsoids are displayed at 30% probability and hydrogen atoms are omitted for clarity.^[46]

prepared by co-complexation of $[\text{NaN}(\text{SiMe}_3)\text{Dipp}]^{[27]}$ and $\text{Fe}(\text{HMDS})_2$ and isolated in an improved 71% yield.

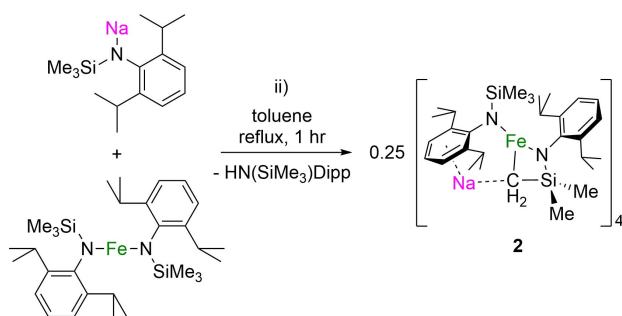
Featuring the same planar four-membered $\{\text{NaNFeN}\}$ ring as I,^[28] where both metals connect via two HMDS bridges, the new $\text{N}(\text{SiMe}_3)\text{Dipp}$ ligand occupies the third (terminal) coordination site on iron. Consistent with a ferrate constitution this terminal Fe–N bond distance $[\text{Fe1–N3}, 1.9727(18) \text{ \AA}]$ is noticeably longer than that reported by Power for $\text{Fe}\{\text{N}(\text{SiMe}_3)\text{Dipp}\}_2$ $[1.853(1) \text{ \AA}]$.^[14] Being coordinatively unsaturated, the solvent-free Na centre also engages in two anagostic interactions with two methyls belonging to the HMDS bridges $[2.741(3) \text{ and } 2.758(3) \text{ \AA}]$ as well as with the *para* carbon on the Dipp ring of an adjacent unit $[\text{Na–C19 } 2.924(3) \text{ \AA}]$, to give overall a 1D polymeric arrangement (Figure 1). While 1 is isolated as a homogeneous and pure crystalline product (see Supporting Information), its ^1H NMR spectra in C_6D_6 and d_8 -toluene proved to be particularly complex. Along with a new set of signals, some of which can be attributed to 1, by comparing these spectra with those from its precursors we can also observe the presence of $\text{Fe}\{\text{N}(\text{SiMe}_3)\text{Dipp}\}_2$, NaHMDS and $[\text{NaFe}(\text{HMDS})_3]$ (I) (see Supporting Information for details). These findings are consistent with a redistribution process that we tentatively propose in Scheme 1. Our previous reactivity and computational studies on heteroleptic sodium ferrates containing both HMDS and TMP groups have shown that in solution $[\text{NaFe}(\text{TMP})(\text{HMDS})_2]$ is actually in equilibrium with their homoleptic analogues $[\text{NaFe}(\text{HMDS})_3]$ (I) and $[\text{NaFe}(\text{TMP})_3]$.^[23] A similar process can be proposed to occur for 1 although in this case the steric demand imposed by the $\text{N}(\text{SiMe}_3)\text{Dipp}$ ligand could favour the cleavage of putative complex $[\text{NaFe}(\text{HMDS})\{\text{N}(\text{SiMe}_3)\text{Dipp}\}_2]$ into its single-metal components NaHMDS and complex $\text{Fe}\{\text{N}(\text{SiMe}_3)\text{Dipp}\}_2$ which can be detected spectroscopically (Scheme 1 and S13 in Supporting Information). It should also be noted that Mulvey has reported that related Na and K magnesiate complexes $[\text{M}'\text{Mg}\{\text{N}(\text{SiMe}_3)\text{Dipp}\}_2(n\text{Bu})]_\infty$ undergo redistribution in d_8 -THF solution furnishing the relevant alkali-metal amide and $[\text{M}'\text{N}(\text{SiMe}_3)\text{Dipp}]$ and $\text{BuMg}\{\text{N}(\text{SiMe}_3)\text{Dipp}\}$.^[27] Interestingly in our case, on dissolving isolated crystals of 1 in d_8 -THF the redistribution process depicted in Scheme 1 is suppressed, as evidenced by ^1H NMR data, which reveal six paramagnetically broadened and shifted resonances, ranging from 37.02 to -25.38 ppm, consistent with the retention of heterobimetallic complex 1 (Figure S14 in Supporting Information).



Scheme 1. Proposed redistribution process present in C_6D_6 or d_8 -toluene solutions at room temperature for 1.

Since this transamination approach resulted in only one HMDS group in **1** undergoing exchange, we next attempted the co-complexation of $[\text{NaN}(\text{SiMe}_3)\text{Dipp}]$ and $[\text{Fe}\{\text{N}(\text{SiMe}_3)\text{Dipp}\}_2]$. This is a simple, versatile method widely used in alkali-metal ate chemistry^[29,30] that has already proved to be also effective for ferrate complexes.^[20,28,31,32] That said, on this occasion, mixing equimolar amounts of the sodium and iron amides at ambient temperature in hexane or benzene proved unsuccessful, affording only the unreacted starting materials. However, when the reaction mixture was refluxed in toluene for over one hour, a colour change was observed from a bright orange suspension to a deep red/brown solution, which upon slow cooling yielded a crop of dark red crystals of $[\text{NaFe}\{\text{N}(\text{SiCH}_2\text{Me}_2)\text{Dipp}\}\{\text{N}(\text{SiMe}_3)\text{Dipp}\}]_4$ (**2**) (Scheme 2 and Figure 2) in a 65% yield.

X-ray crystallographic studies established the unique cyclic tetrameric structure of **2**, made up of four $[\text{NaFe}\{\text{N}(\text{SiCH}_2\text{Me}_2)\text{Dipp}\}\{\text{N}(\text{SiMe}_3)\text{Dipp}\}]$ units which aggregate via π -arene interactions of one Na with the Dipp ring of a neighbouring unit, which coordinates in either an η^3 - or η^2 -fashion for Na1 and Na2 respectively (see Figure 2). In each monomer one $\text{N}(\text{SiMe}_3)\text{Dipp}$ group of the Fe *bis*(amide) precursor has been laterally deprotonated at the Me position of one SiMe_3 group, furnishing a dianionic $\text{N}\{\text{CH}_2\text{SiMe}_2\}\text{Dipp}$ ligand. This fragment coordinates



Scheme 2. Synthesis of $[\text{NaFe}\{\text{N}(\text{SiCH}_2\text{Me}_2)\text{Dipp}\}\{\text{N}(\text{SiMe}_3)\text{Dipp}\}]_4$ (**2**).

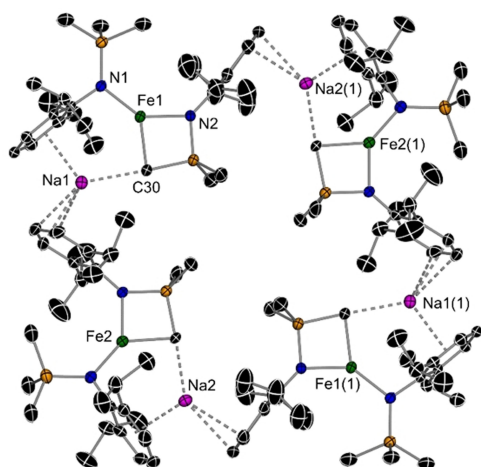


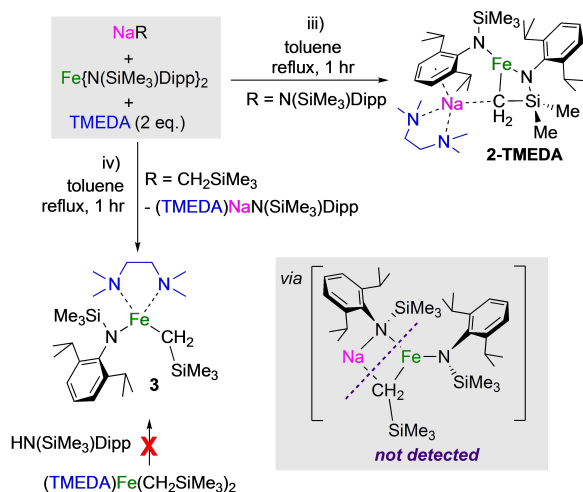
Figure 2. Cyclic tetrameric structure of $[\text{NaFe}\{\text{N}(\text{SiCH}_2\text{Me}_2)\text{Dipp}\}\{\text{N}(\text{SiMe}_3)\text{Dipp}\}]_4$ (**2**). Ellipsoids are displayed at 30% probability and hydrogen atoms are omitted for clarity.^[46]

to Fe in a chelating fashion via its CH_2 and N groups giving rise to a planar four-membered $\{\text{FeCSiN}\}$ ring [sum of internal angles, 359.72°]. Fe completes its distorted trigonal planar geometry [sum of internal angles around Fe1 = 359.87° , ranging from $84.19(15)$ to $140.50(13)^\circ$] by binding terminally to the remaining $\text{N}(\text{SiMe}_3)\text{Dipp}$ amide. The Fe–N bond distances in **2** [ranging from $1.934(3)$ to $1.944(3)$ Å] are slightly elongated than those found in $\text{Fe}\{\text{N}(\text{SiMe}_3)\text{Dipp}\}_2$ [$1.8532(13)$ Å]. Contrastingly Na does not coordinate to any of these N atoms, preferring instead to bind to the newly formed CH_2 fragment [mean Na–C bond length, 2.571 Å] as well as π -engaging with the Dipp group of the amide ligand within the same monomeric unit in an η^6 -fashion.

The ^1H NMR spectrum of **2** recorded in d_8 -toluene displays nine paramagnetically shifted and broadened resonances between -43.65 and 55.60 ppm. Unfortunately, due to a number of overlapping resonances and distortion present in the baseline (arising from its inherent paramagnetic character), integration of the resonances and a meaningful assignment is not possible. The solution magnetic moment of **2** was measured via the Evans method^[33–35] at $4.72 \mu_{\text{B}}$, marginally lower than the spin-only value of $4.90 \mu_{\text{B}}$, for an $S = 2$ iron(II) centre.

Lateral C–H bond activation of the SiMe_3 on the $\text{N}(\text{SiMe}_3)\text{Dipp}$ amide has been previously documented for single metal chromium complexes in the +2 and +3 oxidation states.^[14,36] This reactivity has been attributed to the large steric demands of the relevant putative Cr amides, although these species cannot be detected in solution. Related to these findings the intramolecular deprotonation of $\text{N}(\text{SiMe}_3)\text{Dipp}$ has also been reported with rare-earth metals $\text{Gd}^{[37]}$ and $\text{Tb}^{[38]}$ containing CH_2SiMe_3 groups, where one of these alkyls groups acts as a base, with subsequent release of SiMe_4 . A similar scenario can be proposed for **2**, whose formation can be attributed to the steric incompatibility between the two single metal components which precludes their co-complexation at room temperature. Using more forcing conditions (1 h at reflux in toluene) may lead to the formation of a putative *tris*(amide) sodium ferrate as a short-lived species, with an Fe center very sterically crowded, which eventually will undergo intramolecular lateral metallation of one of its $\text{N}(\text{SiMe}_3)\text{Dipp}$ groups. In this regard, within alkali-metal ate chemistry Mulvey has noted the sterically-induced intramolecular deprotonation of the bulky amide TMP at one of its Me groups in potassium aluminate complexes.^[39] Other examples include the metallation of neutral chelating N-donors such as TMEDA or PMDETA in alkali-metal gallates.^[40] In our case we found that when the reaction of $[\text{NaN}(\text{SiMe}_3)\text{Dipp}]$ and $[\text{Fe}\{\text{N}(\text{SiMe}_3)\text{Dipp}\}_2]$ was carried out in the presence of TMEDA (Scheme 3, iii), lateral metallation of $\text{N}(\text{SiMe}_3)\text{Dipp}$ is still preferred affording $[(\text{TMEDA})\text{NaFe}\{\text{N}(\text{SiCH}_2\text{Me}_2)\text{Dipp}\}\{\text{N}(\text{SiMe}_3)\text{Dipp}\}]$ (**2-TMEDA**) as established by X-ray crystallography (see Figure S5 in Supporting Information). In this case TMEDA is left intact, acting as a neutral chelating donor to Na favouring the formation of a monomeric version of **2**.

Interestingly, replacing $[\text{NaN}(\text{SiMe}_3)\text{Dipp}]$ by alkyl $[\text{NaCH}_2\text{SiMe}_3]$ which *a priori* can also be expected to be a stronger metallating reagent, in the presence of two equiv-



Scheme 3. Syntheses of [(TMEDA)NaFe{N(SiMe₃)Dipp}{N(SiMe₃)Dipp}] (2-TMEDA) (iii) and [(TMEDA)Fe{N(SiMe₃)Dipp}{CH₂SiMe₃}] (3) (iv).

alents of TMEDA led to the isolation of a mixture of the monometallic products [(TMEDA)Na{N(SiMe₃)Dipp}]^[27] and [(TMEDA)Fe{N(SiMe₃)Dipp}{CH₂SiMe₃}] (3) (Scheme 3, iv). The same outcome was found when the reaction was carried out under refluxing conditions in toluene (see Supporting Information for details). The structure of **3** was determined by X-ray crystallographic studies, (Figure 3, LHS). The Fe centre resides in a highly distorted tetrahedral environment [angles around Fe ranging from 79.79(4) to 137.59(5)°], comprising three N atoms (two from the TMEDA donor and one from the amide) and the methylene C from the CH₂SiMe₃. Its ¹H NMR spectrum in C₆D₆ displays a number of broad resonances between 77.22 and –31.33 ppm.

It should be noted that attempts to prepare **3** rationally via deprotonation of the amine HN(SiMe₃)Dipp by iron alkyl [(TMEDA)Fe(CH₂SiMe₃)₂]^[20] were unsuccessful yielding only the unreacted starting materials, illustrating the low kinetic basicity of these alkyl groups when bound to Fe. Formation of **3** can be rationalised considering the initial formation of a mixed alkyl/amide sodium ferrate [NaFe(CH₂SiMe₃){N(SiMe₃)Dipp}₂] which undergoes redistribution into [(TMEDA)Na{N(SiMe₃)Dipp}] and **3** (Scheme 3, iv). These findings offer further support for the

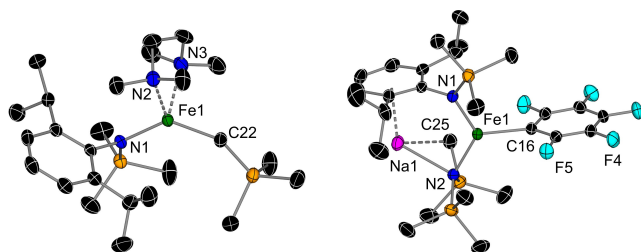


Figure 3. Molecular structure of [(TMEDA)Fe{N(SiMe₃)Dipp}{CH₂SiMe₃}] (3) (left) and asymmetric unit of polymeric [Na{N(SiMe₃)Dipp}{HMDS}Fe(C₆F₅)]_∞ (4) (right). Ellipsoids are displayed at 50% probability and hydrogen atoms are omitted for clarity.^[46]

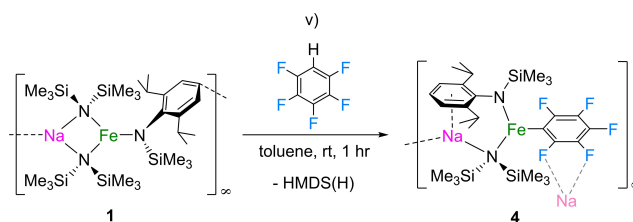
formation of **2** and **2-TMEDA** being driven by the steric incompatibility of its single-metal components rather than the basic capabilities of the sodium reagent employed.

Reactivity studies: assessing ferration of C₆F₅H and pyridine

Next we turned our attention towards investigating the reactivity of sodium ferrates **1** and **2** in Fe–H exchange processes. Our previous studies in this area have demonstrated reactions to be strongly dependent on the nature of the amide employed.^[23] Pentafluorobenzene (C₆F₅H) and pyridine (py) were chosen as model substrates. The former is highly activated in terms of pK_a value of its sole H centre,^[41] whereas the latter is a sensitive electron-deficient substrate for which metallation using conventional polar organometallics can be particularly challenging due to the fragility of their metallated intermediates as well as the difficulty in controlling the regioselectivity of the metal–H exchange.^[42–44]

Focusing first on C₆F₅H, addition of 1 equivalent of this substrate to a toluene solution of **1** produced an instant colour change in the solution from bright orange to pale yellow and the emergence of a light coloured precipitate. Gentle heating to obtain a solution followed by slow cooling to 5 °C furnished large pale pink crystals of [Na{N(SiMe₃)Dipp}{HMDS}Fe(C₆F₅)]_∞ (**4**) in a 57% crystalline yield (Scheme 4 and Figure 3, RHS).

X-ray crystallographic studies of **4** confirmed that the formal ferration of pentafluorobenzene has occurred, replacing one HMDS group in **1**. The newly generated aryl coordinates terminally to Fe, whereas Na and Fe remain connected by HMDS and N(SiMe₃)Dipp bridges. Interestingly, the latter coordinates to both metals in a distinct manner, similar to what has been observed in **2**. It forms a strong terminal Fe–N bond [1.9615(10) Å], whereas it π-engages with the softer Na in a η⁶-fashion with its aromatic ring (Figure 3, RHS). The coordination sphere of Na is completed by an anagostic interaction with a methyl group from HMDS and two further electrostatic contacts to F atoms of a neighbouring unit. The latter propagate a 1D polymeric chain structure for **4** (see Supporting Information for details). In *d*₈-toluene solution the ¹H NMR spectrum of **4** shows six broad resonances between 43.38 and –43.84 ppm. While its paramagnetic character makes difficult the unambiguous assignment of these signals, this is consistent with the presence of **4** as a single species in solution. Importantly none of these resonances correspond to those of Fe{N(SiMe₃)Dipp}₂, thus it



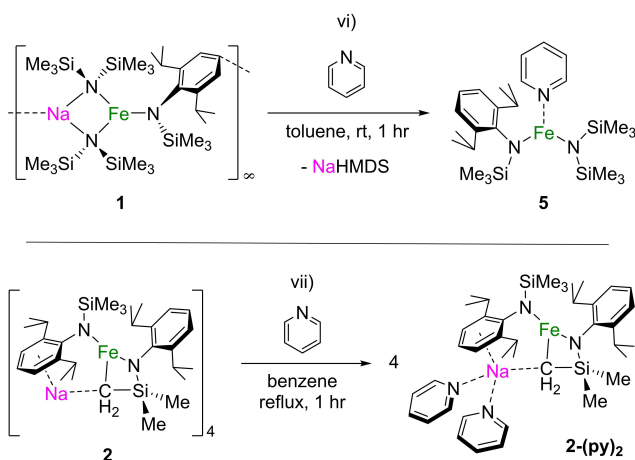
Scheme 4. Synthesis of [Na{N(SiMe₃)Dipp}{HMDS}Fe(C₆F₅)]_∞ (**4**).

appears **4** is stable in solution and not susceptible to the ligand redistribution equilibria observed with **1**.

Formation of **4** suggests that, despite the presence of several species in solution when **1** is dissolved in toluene (Scheme 1, see above) ferration of C_6F_5H occurs via heteroleptic sodium ferrate **1** with subsequent elimination of HMDS(H). It should also be noted that the ferration of pentafluorobenzene by **1** is synergistic in origin since $[Fe\{N(SiMe_3)Dipp\}_2]$ on its own cannot selectively deprotonate this substrate; whereas the stronger base NaHMDS metallates this substrate albeit non-selectively generating a mixture of decomposition products including saline NaF. Formation of **4** can be envisaged to occur via a similar mechanism to that we have recently reported for $[NaFe(HMDS)_3]$ (**I**),^[23] with initial coordination of C_6F_5H to Na in **1** which induces the shift of one bridging HMDS amide to Na, facilitating the Na–H exchange which is immediately followed by a fast intramolecular trapping of the C_6F_5 aryl anion by the Fe(II) centre (see Scheme S1 in Supporting Information).

Unfortunately, experiments assessing the metallating ability of **2** were inconclusive. Addition of C_6F_5H to complex **2** induced a colour change to an opaque deep purple solution, however this led to the formation of an intractable mixture of products which could not be confidently assigned by 1H NMR spectroscopy and that failed to deposit any crystalline material for further analysis.

Turning our attention to pyridine, reaction with $[NaFe(HMDS)_3]$ (**I**) fails to induce its metallation. In contrast, with the more basic and sterically demanding sodium amide $[NaTMP]$ in combination with $[Fe(HMDS)_2]$, regioselective ferration of pyridine with preference for the uncommon 3-position is accomplished.^[23] Addition of one equivalent of pyridine to a toluene solution of **1** led to the formation of a bright yellow solution (Scheme 5, top) which on cooling deposited crystals of heteroleptic iron amide $[(py)Fe\{N(SiMe_3)Dipp\}(HMDS)]$ (**5**) (Scheme 5, top). The by-product from this reaction, NaHMDS, could be removed via exchange of toluene by pentane and filtering the cooled solution, affording **5** in a 69% isolated yield.



Scheme 5. Top: Synthesis of $[(py)Fe\{N(SiMe_3)Dipp\}(HMDS)]$ (**5**). Bottom: Synthesis of $[(py)_2NaFe\{N(SiCH_2Me_2)Dipp\}\{N(SiMe_3)Dipp\}]$ (**2-(py)₂**).

A monomer in the solid state, **5** (Figure 4, LHS) comprises a trigonal planar Fe centre coordinated by three N atoms (sum of angles = 359.98°), with N1 and N2 belonging to the amide groups $N(SiMe_3)Dipp$ and HMDS, respectively [Fe–N bond distances, 1.9242(19) and 1.939(2) Å, respectively]; while N3 is part of a neutral pyridine donor molecule [Fe1–N3, 2.122(2) Å]. The structure of **5** compares well with that of the pyridine adducts of the parent amides $[Fe(HMDS)_2]$ and $[Fe\{N(SiMe_3)Dipp\}_2]$ previously reported by Power.^[12,14] It should be noted that these compounds were prepared by reacting directly the relevant Fe(II) amide with pyridine; whereas here we start from a heteroleptic sodium ferrate **1**. Two interesting conclusions can be inferred from these findings. First, that ferrate **1** containing the bulky $N(SiMe_3)Dipp$ is not basic enough to promote the metallation of the less activated substrate pyridine and second, that its coordination to this ferrate as a neutral $2e^-$ donor induces its cleavage into two monometallic species (different to its original monometallic precursors) namely $[NaHMDS]$ and heteroleptic Fe *bis*(amide) **5**.

Metallation of pyridine did not occur either when reacted with compound **2**. Addition of 1 equivalent of pyridine to a benzene solution of **2** and refluxing for 1 h produced the crystalline coordination adduct $[(py)_2NaFe\{N(SiCH_2Me_2)Dipp\}\{N(SiMe_3)Dipp\}]$ (**2-(py)₂**) (Scheme 4, bottom and Figure 4, RHS). Despite the more forceful reaction conditions and the presence of a dianionic alkyl/amide ligand in **2**, the H atoms on the heterocycle are left untouched. Instead, two equivalents of pyridine coordinate to the sodium atom deaggregating the tetrameric structure of **2** giving a similar monomeric motif to the one observed when the reaction is carried out in the presence of TMEDA (Scheme 3 and Supporting Information). Compound **2-(py)₂** was fully characterized by X-ray crystallographic studies (Figure 4), 1H NMR, FTIR spectroscopy, and elemental analysis (see Supporting Information for details).

It should also be noted that sodium ferrates **1** and **2** are stable in toluene and benzene solutions and no metallation of these arenes was observed even under forcing reaction conditions. This contrast with our previous work using NaTMP/ $[Fe(HMDS)_2]$ combinations which deprotonate these solvents almost instantaneously at room temperature.

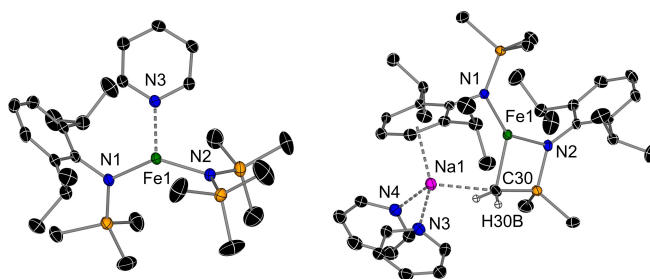


Figure 4. Molecular structures of $[(py)Fe\{N(SiMe_3)Dipp\}(HMDS)]$ (**5**) (left) and $[(py)_2NaFe\{N(SiCH_2Me_2)Dipp\}\{N(SiMe_3)Dipp\}]$ (**2-(py)₂**) (right). Ellipsoids are displayed at 30% probability and hydrogen atoms (except methylene protons) are omitted for clarity.^[46]

Conclusion

Systematically studying the synthesis of sodium ferrates containing the highly sterically demanding amide N(SiMe₃)Dipp, has provided new insights on their stability, structural diversity and reactivity. The large steric bulk imposed by this amide has precluded the isolation of a homoleptic *tris*(amido) sodium ferrate, when trying a transamination approach, employing an excess of the amine HN(SiMe₃)Dipp and [NaFe(HMDS)₃] allowed for only one of three HMDS groups to be exchanged. Alternatively, attempts to force co-complexation of the Na and Fe single-metal N(SiMe₃)Dipp amides lead to the formation of a novel activation product, resulting from lateral metallation of one Me from the SiMe₃ group in [Fe{N(SiMe₃)Dipp}₂], apparently driven by the steric incompatibility between [Na{N(SiMe₃)Dipp}] and [Fe{N(SiMe₃)Dipp}₂] rather than the basic character of the sodium amide. This was indirectly confirmed since using the more basic sodium partner [NaCH₂SiMe₃], where no internal metallation is observed. The reactivity of these new heterobimetallic complexes towards Fe–H exchange processes has been explored using pentafluorobenzene and pyridine as model substrates. More activated pentafluorobenzene can be selectively ferrated by heteroleptic [Na(HMDS)₂Fe{N(SiMe₃)Dipp}]_∞ (1) via one HMDS group whereas with pyridine, elimination of [NaHMDS] is observed yielding pyridine-solvated heteroleptic iron amide [(py)Fe{N(SiMe₃)Dipp}(HMDS)].

Collectively these findings advance the understanding on how ligand effects can greatly affect the structure and therefore the reactivity and stability of alkali-metal ferrates. They also showcase the rich structural diversity of these systems. All the new sodium ferrates described in this work are made up by a combination of strong Fe–N and Fe–C bonds which provide the foundations of the structure to which the Na atoms are affixed via a combination of ancillary bonds such as anagostic/π-interactions with the SiMe₃ and Dipp substituents respectively or via Na···F dative contacts. These ancillary bonds facilitate the formation of more intricate oligomeric structures. Originating from the cooperativity of combining sodium and iron in the same structure, this chemistry clearly fits into the category of synergistic alkali metal mediation, a theme recently reviewed for main group systems,^[45] that offers vast scope for future development in transition metal chemistry.

Experimental Section

Full experimental and characterisation details can be found in the Supporting Information. Deposition Numbers 2091632 (1), 2091633 (2), 2091634 (2-TMEDA), 2091635 (3), 2091636 (4), 2091637 (5), 2091638 (2-(py)₂) contain the supplementary crystallographic data for this paper. These data are provided free of charge by the joint Cambridge Crystallographic Data Centre and Fachinformationszentrum Karlsruhe Access Structures service.

Acknowledgements

We thank the University of Bern and the SNF (188573) for the generous sponsorship of this research. The X-ray crystal structure determination service unit of the Department of Chemistry, Biochemistry and Pharmaceutical Sciences of the University of Bern is acknowledged for measuring, solving, refining and summarizing the structures of compounds 2–5. The Synergy diffractometer was partially funded by the Swiss National Science Foundation (SNF) within the R'Equip programme (project number 206021_177033). We also thank Robert E. Mulvey from the University of Strathclyde for his valuable comments and discussions and Martin Albrecht and Albert Farré from the University of Bern for their assistance with FTIR measurements. Open access funding provided by Universität Bern.

Conflict of Interest

The authors declare no conflict of interest.

Keywords: cooperative effects · ferrates · metallation · sodium bimetallic compounds

- [1] P. P. Power, *Chem. Rev.* **2012**, *112*, 3482–3507.
- [2] D. L. J. Broere, I. Čorić, A. Brosnahan, P. L. Holland, *Inorg. Chem.* **2017**, *56*, 3140–3143.
- [3] A. Eichhöfer, Y. Lan, V. Mereacre, T. Bodenstein, F. Weigend, *Inorg. Chem.* **2014**, *53*, 1962–1974.
- [4] T. Bodenstein, A. Eichhöfer, *Dalton Trans.* **2019**, *48*, 15699–15712.
- [5] C. G. Werncke, L. Vendier, S. Sabo-Etienne, J.-P. Sutter, C. Pichon, S. Bontemps, *Eur. J. Inorg. Chem.* **2017**, *2017*, 1041–1406.
- [6] R. A. Layfield, J. J. W. McDouall, M. Scheer, C. Schwarzmaier, F. Tuna, *Chem. Commun.* **2011**, *47*, 10623–5.
- [7] B. M. Day, T. Pugh, D. Hendriks, C. F. Guerra, D. J. Evans, F. M. Bickelhaupt, R. A. Layfield, *J. Am. Chem. Soc.* **2013**, *135*, 13338–41.
- [8] T. N. Gieshoff, U. Chakraborty, M. Villa, A. Jacob von Wangelin, *Angew. Chem. Int. Ed.* **2017**, *56*, 3585–3589; *Angew. Chem.* **2017**, *129*, 3639–3643.
- [9] R. Araake, K. Sakadani, M. Tada, Y. Sakai, Y. Ohki, *J. Am. Chem. Soc.* **2017**, *139*, 5596–5606.
- [10] J. Yang, T. D. Tilley, *Angew. Chem. Int. Ed.* **2010**, *49*, 10186–10188; *Angew. Chem.* **2010**, *122*, 10384–10386.
- [11] C. G. Werncke, P. C. Bunting, C. Duhayon, J. R. Long, S. Bontemps, S. Sabo-Etienne, *Angew. Chem. Int. Ed.* **2015**, *54*, 245–248; *Angew. Chem.* **2015**, *127*, 247–250.
- [12] M. M. Olmstead, P. P. Power, S. C. Shoner, *Inorg. Chem.* **1991**, *30*, 2547–2551.
- [13] J. M. Zadrozny, M. Atanasov, A. M. Bryan, C. Y. Lin, B. D. Reinken, P. P. Power, F. Neese, J. R. Long, *Chem. Sci.* **2013**, *4*, 125–138.
- [14] C.-Y. Lin, J.-D. Guo, J. C. Fettinger, S. Nagase, F. Grandjean, G. J. Long, N. F. Chilton, P. P. Power, *Inorg. Chem.* **2013**, *52*, 13584–13593.
- [15] C.-Y. Lin, J. C. Fettinger, F. Grandjean, G. J. Long, P. P. Power, *Inorg. Chem.* **2014**, *53*, 9400–9406.
- [16] R. Weller, I. Müller, C. Duhayon, S. Sabo-Etienne, S. Bontemps, C. G. Werncke, *Dalton Trans.* **2021**, *50*, 4890–4903.
- [17] M. I. Lipschutz, T. Chantarojsiri, Y. Dong, T. D. Tilley, *J. Am. Chem. Soc.* **2015**, *137*, 6366–6372.
- [18] R. J. Witzke, D. Hait, M. Head-Gordon, T. D. Tilley, *Organometallics* **2021**, *40*, 1758–1764.
- [19] R. J. Witzke, D. Hait, K. Chakarawet, M. Head-Gordon, T. D. Tilley, *ACS Catal.* **2020**, *10*, 7800–7807.
- [20] P. Alborés, L. M. Carrella, W. Clegg, P. García-Álvarez, A. R. Kennedy, J. Klett, R. E. Mulvey, E. Rentschler, L. Russo, *Angew. Chem. Int. Ed.* **2009**, *48*, 3317–3321; *Angew. Chem.* **2009**, *121*, 3367–3371.

- [21] S. H. Wunderlich, P. Knochel, *Angew. Chem. Int. Ed.* **2009**, *48*, 9717–9720; *Angew. Chem.* **2009**, *121*, 9897–9900.
- [22] L. C. H. Maddock, T. Nixon, A. R. Kennedy, M. R. Probert, W. Clegg, E. Hevia, *Angew. Chem. Int. Ed.* **2018**, *57*, 187–191; *Angew. Chem.* **2018**, *130*, 193–197.
- [23] L. C. H. Maddock, M. Mu, A. R. Kennedy, M. García-Melchor, E. Hevia, *Angew. Chem. Int. Ed.* **2021**, *60*, 15296–15301; *Angew. Chem.* **2021**, *133*, 15424–1542.
- [24] L. C. H. Maddock, A. Kennedy, E. Hevia, *Chimia* **2020**, *74*, 866–870.
- [25] M. Uzelac, R. E. Mulvey, *Chem. A Eur. J.* **2018**, *24*, 7786–7793.
- [26] L. C. H. Maddock, I. Borilovic, J. McIntyre, A. R. Kennedy, G. Aromí, E. Hevia, *Dalton Trans.* **2017**, *46*, 6683–6691.
- [27] M. Á. Fuentes, A. Zabala, A. R. Kennedy, R. E. Mulvey, *Chem. A Eur. J.* **2016**, *22*, 14968–14978.
- [28] L. C. H. Maddock, T. Cadenbach, A. R. Kennedy, I. Borilovic, G. Aromí, E. Hevia, *Inorg. Chem.* **2015**, *54*, 9201–9210.
- [29] R. E. Mulvey, *Acc. Chem. Res.* **2009**, *42*, 743–55.
- [30] S. D. Robertson, M. Uzelac, R. E. Mulvey, *Chem. Rev.* **2019**, *119*, 8332–8405.
- [31] S. N. König, D. Schneider, C. Maichle-Mössmer, B. M. Day, R. A. Layfield, R. Anwender, *Eur. J. Inorg. Chem.* **2014**, *2014*, 4302–4309.
- [32] S. A. Sulway, D. Collison, J. J. W. McDouall, F. Tuna, R. A. Layfield, *Inorg. Chem.* **2011**, *50*, 2521–6.
- [33] D. F. Evans, *J. Chem. Soc.* **1959**, 2003.
- [34] E. M. Schubert, *J. Chem. Educ.* **1992**, *69*, 62.
- [35] C. Piguet, *J. Chem. Educ.* **1997**, *74*, 815–816.
- [36] H. J. Liu, I. C. Cai, A. Fedorov, M. S. Ziegler, C. Copéret, T. D. Tilley, *Helv. Chim. Acta* **2016**, *99*, 859–867.
- [37] Y. Luo, M. Nishiura, Z. Hou, *J. Organomet. Chem.* **2007**, *692*, 536–544.
- [38] L. Yunjie, C. Jue, M. Honglei, *J. Rare Earth* **2007**, *25*, 554–557.
- [39] B. Conway, A. R. Kennedy, R. E. Mulvey, S. D. Robertson, J. G. Álvarez, *Angew. Chem. Int. Ed.* **2010**, *49*, 3182–3184; *Angew. Chem.* **2010**, *122*, 3250–3252.
- [40] R. McLellan, M. Uzelac, L. J. Bole, J. M. Gil-Negrete, D. R. Armstrong, A. R. Kennedy, R. E. Mulvey, E. Hevia, *Synthesis* **2019**, *51*, 1207–1215.
- [41] K. Shen, Y. Fu, J.-N. Li, L. Liu, Q.-X. Guo, *Tetrahedron* **2007**, *63*, 1568–1576.
- [42] J. Verbeek, A. V. E. George, R. L. P. De Jong, L. Brandsma, *J. Chem. Soc. Chem. Commun.* **1984**, 257–258.
- [43] J. Verbeek, L. Brandsma, *J. Org. Chem.* **1984**, *49*, 3857–3859.
- [44] P. Gros, Y. Fort, P. Caubère, *J. Chem. Soc. Perkin Trans. 1* **1997**, 3597–3600.
- [45] T. X. Gentner, R. E. Mulvey, *Angew. Chem. Int. Ed.* **2021**, *60*, 9247–9262.
- [46] Deposition Numbers 2091632 (1), 2091633 (2), 2091634 (2-TMEDA), 2091635 (3), 2091636 (4), 2091637 (5), 2091638 (2-(py)₂) contain the supplementary crystallographic data for this paper. These data are provided free of charge by the joint Cambridge Crystallographic Data Centre and Fachinformationszentrum Karlsruhe Access Structures service.

Manuscript received: June 28, 2021

Accepted manuscript online: July 29, 2021

Version of record online: September 12, 2021